Available online at www.sciencedirect.com
SCIENCE DIRECT
Journal of Power Sources 157 (2006) 624–629
JOURNAL OF POWER SOURCES
www.elsevier.com/locate/jpowsour

Short communication

Synthesis of zinc sulphide nanoparticles by thiourea hydrolysis and their characterization for electrochemical capacitor applications

M. Jayalakshmi, M. Mohan Rao *

Inorganic Chemistry Division, Indian Institute of Chemical Technology, Hyderabad 500007, India

Received 16 May 2005; accepted 11 August 2005
Available online 13 September 2005

Abstract

A simple method is applied to prepare nanocrystalline ZnS using zinc nitrate and thiourea in aqueous solutions. Cubic sphalerite ZnS is obtained in phase pure form when S/Zn mole ratio is 1 and 2. A mixed phase of hexagonal wurtzite and cubic sphalerite ZnS is obtained when S/Zn mole ratio is 4. Transmission electron microscope and X-ray diffraction confirm the formation of ZnS nanoparticles. These nanoparticles are immobilized on the surface of paraffin impregnated graphite electrode (PIGE) and electrochemical characterization in neutral solutions by cyclic voltammetry revealed that the material is ideal to be used as electrode in electrochemical double layer capacitors. The most singularly interesting result is the voltages observed in 0.1 M LiCl, NaCl, NaI and KI solutions. They are 3.0, 2.7, 2.0 and 1.8 V versus Ag/AgCl and significantly higher than the expected value of 1.23 V (pH ∼ 7) in aqueous medium. Such a large voltages are usually obtained for non-aqueous electrolytes and the present study showed a surprising and significant interesting result that can be owed to the over potentials of $H_2/O_2/Cl_2$ gas evolutions. An attempt to understand these highly significant results in terms of band edge bendings (conduction band and valence band) associated with the positive and negative ion adsorption at the interface of semiconductor ZnS/solution is made.

Keywords: ZnS nanoparticles; Thiourea hydrolysis; Electrochemical double layer capacitance; Cyclic voltammetry; High voltage; Band edge bendings

1. Introduction

ZnS is an important inorganic semiconducting material occurring in nature as cubic sphalerite and hexagonal wurtzite with tetrahedrically bonded Zn^{2+}. At room temperature, hexagonal wurtzite and cubic sphalerite has a wide band gap around 3.5–3.8 eV. The applications of ZnS are numerous to its credit. It is a traditional phosphor material used widely in displays, sensors, solar cells, lasers and electroluminescence. In optoelectronics, it finds use as light emitting diode, reflector, dielectric filter and window material [1]. In view of its technological importance, synthesis of ZnS remains a topic of interest for researchers, as new synthetic routes are being explored to get phase pure material via an economically and technically viable method. Recently, preparation of nanosize ZnS is of particular concern. ZnS nano rods are synthesized by a surfactant assisted soft chemistry method [2]. By electrically driven spray pyrolysis ZnS nanoparticles were prepared from zinc nitrate and thiourea using ethyl alcohol solutions [3]. Microwave and γ-irradiation techniques were applied to prepare ZnS nanocrystals from zinc salts using thioacetamide and thiourea as sulfur source [4,5]. Using a novel electrostatic assisted aerosol jet deposition technique at 450 °C, ZnS films are prepared from an aqueous solution of zinc chloride and thiourea. However, the films showed a mixture of hexagonal and cubic structures and lacked phase purity [6].

Semiconducting nanomaterials are ubiquitous in device electronics, as their charge distribution can be manipulated desirably by applying voltage to perform the logic operations. One such is the present work that deals with electrochemical double layer capacitance of ZnS nanoparticles so that the feasibility of the nanomaterial to be used as electrode for electrochemical capacitor (EC) can be elucidated. Electrochemical capacitors utilize the non-Faradic double layer capacitance of electrode interfaces as a means of storing

* Corresponding author. Tel.: +91 40 27193510; fax: +91 40 27160921.
E-mail address: mandapati@iict.res.in (M.M. Rao).

0378-7753/$ – see front matter © 2005 Elsevier B.V. All rights reserved.
doi:10.1016/j.jpowsour.2005.08.001

electrical energy. Though this concept was initialized and industrialized some 40 years ago, there was a stagnancy in research until recent times; the need for this revival of interest arises due to the increasing demands for electrical energy storage in certain current applications like digital electronic devices, implantable medical devices and stop/start operation in vehicle traction which need very short high power pulses that could be fulfilled by electrochemical capacitors. They are complementary to batteries as they deliver high power density and low energy density. They also have longer cycle life than batteries and possess higher energy density as compared to conventional capacitors. This has led to new concepts of the so-called hybrid charge storage devices in which electrochemical capacitor is interfaced with a fuel cell or a battery [7].

In the present work, we report a simple, single step hydrothermal synthesis of ZnS nanoparticles. The nanophase material is characterized by XRD and TEM. Nano ZnS immobilized on the surface of paraffin impregnated graphite electrode (PIGE) is characterized for electrochemical capacitors using cyclic voltammetric technique in aqueous electrolytes like LiCl, NaCl, KI and NaI. Tremendous over potential for hydrogen evolution in all the neutral electrolyte solutions lead to significantly higher voltages which is unusual for aqueous electrolytes. To understand the origin of these over potentials in the semiconductor ZnS electrode, band edge bendings associated with positive and negative ions adsorption at the interface, analogous to photo electrochemical water splitting by TiO_2 semiconductor to produce hydrogen is visualized [8].

2. Experimental

2.1. Hydrothermal synthesis of ZnS nanoparticles

In a typical experiment (sample A) analar grade $Zn(NO_3)_2{\cdot}6H_2O$ (0.04 moles) and thiourea (0.04 moles) are dissolved in 200 ml of deionized water and the solution was transferred to autoclave SS pressure vessel. The autoclave was programmed to reach 170 °C in 1 h (ramp time) and at this temperature the reaction was kept for 2 h (soak time) with stirring speed of 400 rpm. During the experiment the in situ pressure developed was 15 atm. When autoclave temperature reached to RT, the solution with precipitate (pH ∼ 8) was filtered and washed with distilled water to get neutral pH. The white filtered solid was dried overnight in oven at 120 °C. With an aim to see the effect of excess thiourea on the final product, two more experiments with S/Zn ratios of 2.0 (sample B) and 4.0 (sample C) were done under similar experimental conditions.

2.2. Instrumentation

Powder X-ray diffraction (XRD) data of the samples were obtained using X-ray diffractometer of Siemens D 5000 with Bragg–Brentano geometry having Cu Kα radiation (40 kV, 30 mA), fixed slits and a graphite secondary monochromater. The samples were scanned for 2θ values ranging from 2° to 70° with a scan speed of 1° min^{-1}. Transmission electron microscope (TEM) photographs were obtained using Tecnai-12 FEI instrument. X-ray Photoelectron Spectroscopy (XPS) measurements were conducted with Kratos XPS Axis 165 spectrometer, equipped with a hemispherical energy analyzer. The non-monochromatized Mg Kα X-ray source ($h\nu = 1253.6$ eV) was operated at 5 kV and 15 mA, with pass energy of 80 eV and a step of 0.1 eV. The samples were degassed for several hours in the XPS chamber to minimize air contamination to sample surface. Electrochemical experiments were conducted with a PGSTAT 30 Autolab system (Ecochemie, The Netherlands). The reference electrode was an Ag/AgCl (3M KCl) electrode and the counter electrode was a platinum foil supplied along with the instrument. The working electrode was a nano ZnS immobilized on the surface of PIGE. In our earlier works, we have employed this technique successfully to evaluate $LiNiO_2$, $LiCoO_2$ and $LiMnO_2$ electrode materials for reversible battery applications and nano SnS and SnO for super capacitors [9].

3. Results and discussion

3.1. Material characterization

The powder X-ray diffraction (XRD) patterns of the as-prepared samples A (S/Zn = 1.0), B (2.0) and C (4.0) are shown in Fig. 1. The XRD patterns of the ZnS samples A and B exhibit a single phase sphalerite crystal structure. The three diffraction (1 1 1), (2 2 0) and (3 1 1) planes correspond to cubic crystalline ZnS (JCPDS Card 05-0566). The calculated unit cell parameter $a = 5.319$ Å is lesser than the expected bulk lattice parameter of 5.405 Å. The reason for this anomaly has been attributed to the tetragonal distortion of the unit cell of nanoparticles [10]. The XRD pattern of the sample C shows additional peaks at (1 0 0) and (1 0 1) planes, revealing the presence of 2H hexagonal wurtzite phase with

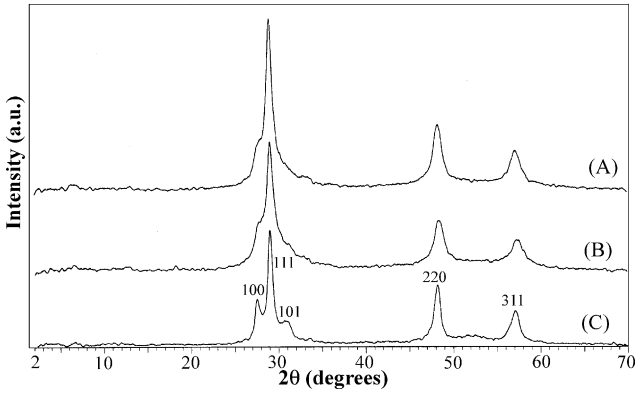

Fig. 1. XRD patterns of ZnS samples A, B and C.

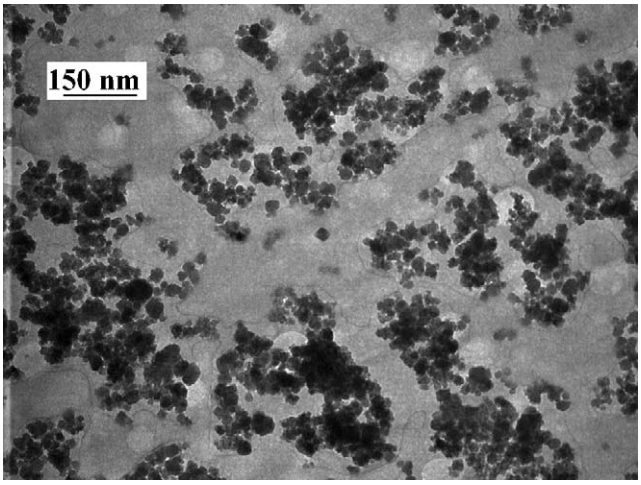

Fig. 2. Transmission electron microscopic image of ZnS.

unit cell parameters $a = 3.741$ and $c = 6.142$ along with the predominant cubic sphalerite ZnS phase [11]. Broadening of the peaks indicates the nanocrystalline nature of the material and the crystallite sizes calculated from the FWHM of diffraction peak (1 1 1) using the Scherrer equation are 9.3, 10.5 and 12.7 nm for samples A, B and C, respectively.

TEM image (Fig. 2) shows the beautifully formed cubic shaped nanoparticles of ZnS (sample A). The tendency to form nanoclusters due to the high surface energy of nanoparticles is an unavoidable phenomenon as observed in the present case. The particles sizes ranges from 15 to 30 nm and the cubic shape of the individual particle was retained irrespective of the size.

The XPS measurements were carried out for sample A (figure not given) and the observed binding energies of Zn $2p_{3/2}$ and Zn $2p_{1/2}$ levels are 1022.47 and 1045.45 eV, respectively, which indicate the presence of zinc in Zn^{2+} form [12]. The binding energies of S $2p_{3/2}$ (162.5 eV) and S $2p_{1/2}$ (163.152 eV) denote the sulfur in S^{2-} form and no other sulfur levels like S^0 and S^{6+} are observed indicating the formation of phase pure ZnS nanomaterial.

3.2. Electrochemical characterization

The cyclic voltammograms (CVs) obtained for nano ZnS (sample A) immobilized on PIGE in 0.1 M LiCl, NaCl, KI, NaI solutions are shown in Figs. 3–6, respectively. They show clearly the rectangular and almost symmetric current–potential characteristics of a capacitor. The reason for the appearance of rectangular shaped CV for a typical capacitive behavior has been well documented [13]. The equivalent circuit of double layer capacitor electrodes can be represented by a serial combination of equivalent series resistance (R) and double layer capacitance (C). The shape of the voltammogram was duly determined by the time constant, τ (RC) of the electrochemical cell. If τ (RC) $\neq 0$, then the shape of the CV would be non-rectangular indicating a current containing a transient part as well as a steady state

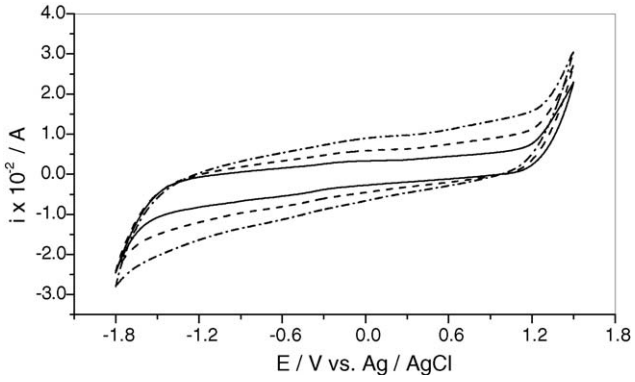

Fig. 3. Cyclic voltammograms of ZnS in 0.1 M LiCl solutions at different scan rates: (—) 20 mV s^{-1}; (- - -) 50 mV s^{-1}; (- · -) 100 mV s^{-1}.

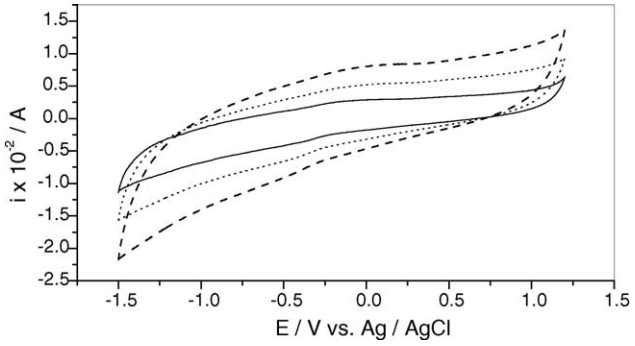

Fig. 4. Cyclic voltammograms of ZnS in 0.1 M NaCl solutions at various scan rates: (—) 20 mV s^{-1}; (···) 50 mV s^{-1}; (- - -) 100 mV s^{-1}.

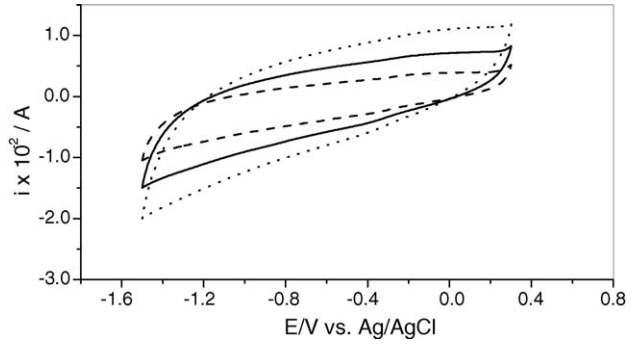

Fig. 5. Cyclic voltammograms of ZnS in 0.1 M KI solutions at various scan rates: (- - -) 20 mV s^{-1}; (—) 50 mV s^{-1}; (···) 100 mV s^{-1}.

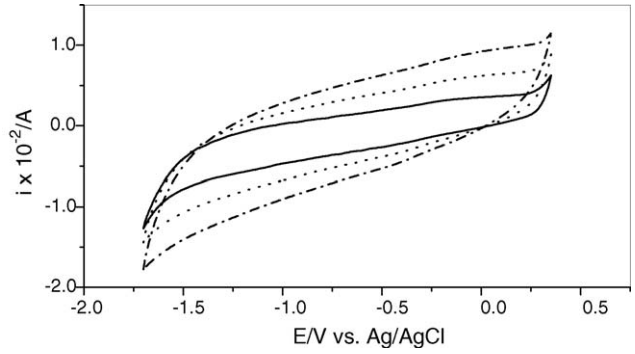

Fig. 6. Cyclic voltammograms of ZnS in 0.1 M NaI solutions at various scan rates: (—) 20 mV s^{-1}; (···) 50 mV s^{-1}; (- - -) 100 mV s^{-1}.

Table 1
Parameters calculated from the cyclic voltammograms of nano ZnS in neutral electrolyte solutions

Electrolyte solutions (0.1 M)	E^{R}_{onset} (V) vs. Ag/AgCl	E^{OX}_{onset} (V) vs. Ag/AgCl	ΔV or E^{CV}_{g} (V)	C_{dl} (F)	
				Q_a	Q_c
LiCl	−1.75	1.35	3.0	14.2	13.3
NaCl	−1.50	1.20	2.7	6.03	6.19
NaI	−1.70	0.35	2.0	6.74	6.64
KI	−1.50	0.30	1.8	3.09	2.83

part. As τ becomes larger, the transient part lasts longer and hence more time is required to charge the capacitor resulting in the collapse of the rectangular current profile. It is clearly evident from the CVs, the nanomaterial acts as a typical capacitor electrode. This is also a characteristic feature of semiconductor electrode permeated with a conductive phase which has the ability to accumulate a large number of injected electron charges in the solid matrix. In the case of ZnS nanoparticles, a combination of several factors such as the nanosize, a good electronic conductivity between particles and the presence of a surrounding equipotential surface played a role which in turn displaces the Fermi level toward the semiconductor conducting band producing a homogeneous increase in the electron concentration in the electrode surface. This increases the electrochemical capacitive behavior as the rate of charge transfer depends on the diffusion of anions and cations towards the ZnS/solution interface and the overlap of the electronic levels in the ZnS with the redox species in the solution [14].

Table 1 presents the parameters obtained from the CVs of nano ZnS for all the electrolyte solutions. Capacitance is expressed as,

$$C = \frac{\mathrm{d}q}{\mathrm{d}E} \text{ or } C = I\frac{\mathrm{d}t}{\mathrm{d}E}$$

For the calculation of specific capacitance ($\mathrm{F\,g^{-1}}$) from CV measurements, the average anodic (Q_a) and cathodic (Q_c) capacitances were calculated from the following expression:

$$C = \left[\frac{i\,(\mathrm{A}) \times t\,(\mathrm{s})}{w\,(\mathrm{g}) \times \Delta E\,(\mathrm{V})}\right]$$

where all the terms has the usual meaning. The difference in weight of the PIGE before and after immobilization gives the mass (w) taken. The capacitive current for both anodic and cathodic scans was obtained from the CVs of slow scan rate ($20\,\mathrm{mV\,s^{-1}}$). Since in the technique of cyclic voltammetry, there is a linear change of potential with time, this being excitation signal, the potential axis simultaneously represents a linear time axis. On integration of the current over time between two potential limits, the charge value, i.e. the numerator of the above equation can be evaluated. The difference between the anodic and cathodic double layer capacitance values was minimal. From the data, it was clear that ZnS performs at its best in LiCl solutions and the opposite in NaI solutions. The reason for this disparity in behavior could be assigned to the high electropositive charge of Li^+ ions and the tendency to form an effective double layer with its heavily hydrated sheath is advantageous as against the Na^+ ion. The fact that the capacitance was lower in NaI solutions as compared to NaCl solutions led us to believe that the counter cations also play a significant role in deciding the performance of ZnS electrode.

Another singularly interesting and significant observation was the high voltages in par with that obtained for non-aqueous electrolytes. It is well known that the potential limits in water as solvent is decided by the hydrogen evolution at the negative end and oxygen evolution at the positive end. In aqueous medium, the H_2 and O_2 gas evolutions occur as per the following equations [15]:

$$2\mathrm{H_2O} + 2\mathrm{e^-} \rightarrow \mathrm{H_2} + 2\mathrm{OH^-},$$
$$E^0\,(\mathrm{pH\,7}) = -0.65\,\mathrm{V\ versus\ Ag/AgCl} \quad (1)$$

$$2\mathrm{H_2O} \rightarrow \mathrm{O_2} + 4\,\mathrm{H^+} + 4\mathrm{e^-},$$
$$E^0\,(\mathrm{pH\,7}) = +0.58\,\mathrm{V\ versus\ Ag/AgCl} \quad (2)$$

Theoretically, this gives a voltage window of 1.23 V. If the decomposition of the water is prolonged on either side due to the experimental conditions, then the potential at which the gas evolution occurs is termed as the over potential. By definition, an over potential is the additional potential (beyond the thermodynamic requirement) needed to drive a reaction at a certain rate. The over potential is not a unique factor but depends on the electrode material and working medium. We believe this over potential phenomenon (as significantly used in solar water splitting) can be used as a guide to understand the high voltages observed for nano ZnS in LiCl and NaCl solutions. It could be seen in LiCl solutions that hydrogen evolution occurs nearly 1100 mV more negative than the thermodynamic potential while the oxygen evolution occurs nearly 770 mV more positive than the thermodynamic potential; this gives a voltage of 3.0 V for LiCl solutions, a noticeably high value in aqueous medium. On similar lines, a voltage of 2.7 V was noted for NaCl solutions. These values were comparable with 2.6–3.0 V obtained for carbon electrodes in acetonitrile with $TEABF_4$ [16]. In KI and NaI solutions, the iodine evolution at the positive end (visible observation), being an under potential evolution led to the lesser voltages.

Zinc sulphide (ZnS) is a well known II–VI, n-type semiconductor with band gap energy of 3.66 eV. This optical band gap poses a similarity to the electrochemical band gap (E^{CV}_{g})

or ΔV which was calculated from the cyclic voltammetric curves by measuring the difference in potential between the anodic and cathodic onset potential values [17]. The anodic and cathodic onset potentials are basically related to the exhaustion of available sites for the adsorbed species [13,14]. A similar observation was reported in an earlier work where a large over potential for hydrogen reduction reaction occurred due to subsequent increase in wt% of ZnS [18]. To understand the origin of these over potentials in the semiconductor ZnS electrode, band edge bendings associated with positive and negative ions adsorption at the interface, analogous to photoelectrochemical water splitting by TiO_2 semiconductor to produce hydrogen have been visualized [8].

The capacitive behavior of semiconductor nanocrystalline electrode in contact with an aqueous electrolyte could be explained based on the potential dependence on the intrinsic capacitance which in turn is related to the distribution of electronic states. It is well known that the flat band potential and therefore, the energetics of the band edges of semiconductor/electrolyte system are controlled by the charges in the Helmholtz inner layer. Any change in charge in that layer changes the measured flat band potential and subsequently the energetics of the band edges. When a semiconductor is exposed to dilute solutions, physisorption or chemisorption of the metal ions would create a layer of charges at the semiconductor surface within the Helmholtz layer. Because of this phenomenon, there exists a constant electrochemical potential between the working and counter electrodes at open-circuit conditions, even as the charge transfer across the interface is zero. Application of external bias to the ZnS electrode lead to the following changes: (1) surface charging changes the potential difference across the Helmholtz layer, producing an upward shift of the CB level; (2) electro neutrality requires that the increase in charge of the particles, due to electrons will be balanced by a corresponding increase in positive ion charge at the ZnS/solution interface; (3) charge accumulation being an indispensable prerequisite to align the band edges, the adsorption of positive ions would shift the band edge (CB) towards positive direction; (4) on the reverse negative scan, the adsorption of negative ions would shift the band edges (VB) towards negative direction.

Fig. 7 shows the idealized changes in CB and VB band edges by adsorption of charged metal ions. A positive shift of 0.2 V in the onset of the photocurrent of hydrogen production due to the specific adsorption of Fe^{2+} ions was reported for titania [8]. It was proven that current onset potential can be assigned to the flat band potential since the onset potential shows the clear pH-dependent shift roughly following the well-known Helmhotlz potential shift (−59 mV per ΔpH 1) for a metal oxide semiconductor electrode. In the presence of double layer capacitance alone, the charging current will start at the flat band potential, becoming constant at a constant scan rate of potential [19]. Thus, understanding of the unusually large voltage window (ΔV) or the electrochemical band gap (E_g^{CV}) of nano ZnS in aqueous neutral electrolyte solutions was done by borrowing the basic ideas from the photo electrochemical conversion of water to produce hydrogen. Negative charging of the electronegative chlorine atoms at the surface causes an upward band bending. It was proved Cl_2 adsorbs dissociatively on titania surface and XPS studies revealed that chlorine is an acceptor like adsorbate with an acceptor level below the Fermi level of the substrate and this results in an negatively charged chlorine at the TiO_2 surface and consequently an upward band bending in its vicinity. Ti sites showed shifts downward consistent with an upward band bending [20]. These observations and relevant earlier works confirm our inference that adsorption of ions at the ZnS/Solution interface positively decides the band edge engineering and thereby the unusually large voltages in aqueous medium.

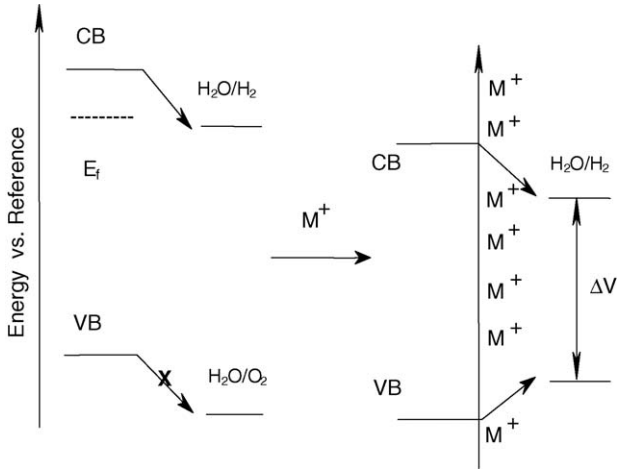

Fig. 7. A hypothetical presentation of band edge bendings due to adsorption of metal ions at the ZnS/solution interface.

4. Conclusions

A simple hydrothermal method is adapted to synthesize nanocrystalline ZnS using zinc nitrate and thiourea in aqueous solutions. By this method, phase pure cubic sphalerite and mixed phase of hexagonal wurtzite and cubic sphalerite ZnS can be synthesized by altering the S/Zn mole ratios. Interestingly, even with excess thiourea no other byproducts of zinc and sulfur other than ZnS were identified. Cyclic voltammetric behavior of nano ZnS in neutral solutions identify the ability to act as electrode for electrochemical capacitor. The unusually large voltages observed for all the neutral solutions studied were in par with that of non-aqueous electrolytes and undoubtedly, this was a very interesting and highly beneficial result in terms of efficiency to deliver power at high rate for a short duration. The capacitance values were attractive and it could be improved by additives of carbon origin. Most preferably, the present work shows a new pathway to identify similar semiconducting materials that can perform as good capacitor electrodes.

Acknowledgement

This work was carried out under CSIR task force project CMM0022.

References

[1] R. Menner, B. Dimmler, R.H. Mauch, H.W. Schock, J. Cryst. Growth 86 (1988) 906;
A.B. Stambouli, S. Hamzaoui, M. Bouderbala, O. Kaid Omar, Appl. Energy 64 (1999) 207;
Q. Zhai, J. Li, J.S. Lewis, K.A. Waldrip, K. Jones, P.H. Holloway, M. Davidson, N. Evans, Thin Sold Films 414 (2002) 105;
A. Yamaga, S. Yoshokawa, H. Kasain, J. Cryst. Growth 86 (1998) 252;
Q. Yitai, S. Yi, X. Yi, C. Qianwang, C. Zuyao, Y. Li, Mater. Res. Bull. 30 (1995) 601.
[2] Q. Zhao, L. Hou, R. Huang, Inorg. Chem. Commun. 6 (2003) 971.
[3] I. Wuled Lenggoro, K. Okuyama, J. Fernández de la Mora, A. Noboru Tohge, J. Aerosol Sci. 31 (2000) 121.
[4] J. Zhu, M. Zhou, J. Xu, X. Liao, Mater. Lett. 47 (2001) 25.
[5] Z. Qiao, X. Yi, Y. Qian, Y. Zhu, Mater. Chem. Phys. 62 (2000) 88.
[6] B. Su, K.L. Choy, J. Mater. Chem. 10 (2000) 949.
[7] R.A. Huggins, Solid State Ionics 34 (2000) 179;
R. Kotz, M. Carlen, Electrochim. Acta 45 (2000) 2483;
G. Gutmann, J. Power Sources 84 (1999) 275.
[8] A. Bansai, J. Beach, R. Collins, O. Khaselev, J.A. Turner, Proceedings of the 1999 U.S. DOE Hydrogen Program Review, NREL/CP-570-26938, 1999.
[9] M. Mohan Rao, M. Jayalaksmi, B. Ramachandra Reddy, S.S. Madhavendra, M. Lakshmi Kantam, Chem. Lett. 34 (2005) 712;
M. Jayalakshmi, M. Mohan Rao, B.M. Choudary, Electrochem. Commun. 6 (2004) 1119;
M. Jayalakshmi, M. Mohan Rao, F. Scholz, Langmuir 19 (2003) 8403.
[10] S.B. Qadri, E.F. Skelton, D. Hsu, A.D. Dinsmore, J. Yang, H.F. Gray, B.R. Ratna, Phys. Rev. B. 60 (1999) 9191.
[11] A.D. Dinsmore, D.S. Hsu, S.B. Qadri, J.O. Cross, T.A. Kennedy, H.F. Gray, B.R. Ratna, J. Appl. Phys. 88 (2000) 4985;
H.T. Evans, E.T. McKnight, Am. Miner. 44 (1959) 1210.
[12] B. Elidrissi, M. Addou, M. Regragui, A. Bougrine, A. Kachouane, J.C. Bernède, Mater. Chem. Phys. 68 (2001) 175.
[13] B.E. Conway, J. Electrochem. Soc. 138 (1991) 1539.
[14] F. Fabregat-Santiago, I. Mora-Sero, G. Garcia-Belmonte, J. Bisquert, J. Phys. Chem. B. 107 (2003) 758.
[15] E. Amouyal, Sol. Energy Mater. Sol. Cells 38 (1995) 249.
[16] M. Ue, K. Ida, S. Mori, J. Electrochem. Soc. 141 (1994) 2989.
[17] M. Al-Ibrahim, A. Konkin, H. Roth, D.A.M. Egbe, E. Klemm, U. Zhokhavets, G. Gobsch, S. Sensfuss, Thin Solid Films 474 (2005) 201.
[18] L.G. Arriaga, A.M. Fernandez, Int. J. Hyd. Energy 27 (2002) 27.
[19] S.R. Morrison (Ed.), Electrochemistry at Semiconductor and Oxidized Metal Electrodes, Plenum Press, New York, 1980, p. 62;
M.S. Lee, I.C. Cheon, Y.I. Kim, Bull. Korean Chem. Soc. 24 (2003) 1155.
[20] M. Batzill, E.L.D. Hebenstreit, W. Hebenstreit, U. Diebold, Chem. Phys. Lett. 367 (2003) 319.